



RESEARCH LETTER

10.1002/2017GL073094

Key Points:

- The first modeling experiment of a full downstate sandy beach sequence is described and analyzed
- Velocity skewness-driven sediment transport is critical to the positive and negative feedback mechanisms
- Downslope gravitational transport acts as an important damping term through morphological diffusivity

Supporting Information:

- Supporting Information S1
- Movie S1
- Figure S1
- Figure S2
- Figure S3
- Figure S4

Correspondence to:

B. Dubarbier,
benjamin.dubarbier@u-bordeaux.fr

Citation:

Dubarbier, B., B. Castelle, G. Ruessink, and V. Marieu (2017), Mechanisms controlling the complete accretionary beach state sequence, *Geophys. Res. Lett.*, 44, 5645–5654, doi:10.1002/2017GL073094.

Received 15 FEB 2017

Accepted 28 MAY 2017

Accepted article online 31 MAY 2017

Published online 15 JUN 2017

Mechanisms controlling the complete accretionary beach state sequence

Benjamin Dubarbier^{1,2}, Bruno Castelle^{1,2}, Gerben Ruessink³, and Vincent Marieu^{1,2}
¹CNRS, UMR EPOC, Pessac, France, ²Université de Bordeaux, UMR EPOC, Bordeaux, France, ³Department of Physical Geography, Faculty of Geosciences, Utrecht University, Utrecht, Netherlands

Abstract Accretionary downstate beach sequence is a key element of observed nearshore morphological variability along sandy coasts. We present and analyze the first numerical simulation of such a sequence using a process-based morphodynamic model that solves the coupling between waves, depth-integrated currents, and sediment transport. The simulation evolves from an alongshore uniform barred beach (storm profile) to an almost featureless shore-welded terrace (summer profile) through the highly alongshore variable detached crescentic bar and transverse bar/rip system states. A global analysis of the full sequence allows determining the varying contributions of the different hydro-sedimentary processes. Sediment transport driven by orbital velocity skewness is critical to the overall onshore sandbar migration, while gravitational downslope sediment transport acts as a damping term inhibiting further channel growth enforced by rip flow circulation. Accurate morphological diffusivity and inclusion of orbital velocity skewness opens new perspectives in terms of morphodynamic modeling of real beaches.

1. Introduction

Nearshore surf zone sandbars, underwater ridges of sand typically in <10 m depth, are ubiquitous along wave-dominated sandy beaches. They act as a natural coastal protection by dissipating wave energy offshore through depth-induced breaking, thus limiting erosion and flooding hazards. Their complex morphology can, however, also enforce localized beach and dune erosion during storms [Thornton *et al.*, 2007; Castelle *et al.*, 2017]. Surf zone sandbars further guide intense ($\mathcal{O}(1\text{ms}^{-1})$) and narrow offshore-directed flows confined in relatively deep rip channels known as rip currents [MacMahan *et al.*, 2006; Dalrymple *et al.*, 2011; Castelle *et al.*, 2016], which are the primary cause of drowning and rescues along surf beaches worldwide [Castelle *et al.*, 2016].

In a pioneering field observation work, Wright and Short [1984] decomposed single-barred intermediate sandy beaches into four states bounded by the fully dissipative and the fully reflective states with, from the most erosive to the most accretive: (1) the longshore bar and trough (LBT) state, sometimes referred to as storm profile, characterized by a continuous alongshore uniform offshore bar; (2) the rhythmic bar and beach (RBB) state characterized by a detached crescentic sandbar; (3) the transverse bar and rip (TBR) state with shore-attached shoals separated by deep rip channels; and (4) the low tide terrace (LTT) characterized by a shore-attached alongshore ridge cut by shallow rip channels. During a full downstate sequence, the sandbar systematically migrates onshore and goes through all the intermediate states from LBT to LTT under low- to moderate-energy wave forcing. Such a full accretionary sequence typically occurs over weeks [e.g., Brander, 1999]. Although such a full sequence has been observed through video monitoring [Ranasinghe *et al.*, 2004; Price and Ruessink, 2011] and laboratory experiment [Michallet *et al.*, 2013], it has never been modeled successfully and the primary driving mechanisms controlling the surf zone sandbar morphological changes are therefore poorly understood.

Surf zone sandbar models can be discriminated into two categories: (1) three-dimensional (3-D) sandbar models and (2) beach profile models. Three-dimensional sandbar models have been developed to study the mechanisms controlling the formation and subsequent nonlinear evolution of TBR and RBB systems starting from an alongshore uniform bar (LBT). These models typically couple a 2-D wave model, a depth-integrated circulation model and a sediment transport model. Using such a modeling approach, regularly spaced rip-channeled morphologies were found to be nearshore morphodynamic instabilities developing as a result

of the positive feedback between waves, flow, sediment transport, and the evolving bathymetry [Falqués *et al.*, 2000]. A variety of such morphodynamic models were subsequently developed and allowed investigating, for instance, the role of preexisting morphologies, wave conditions, or morphological coupling with other bed forms on the nonlinear evolution of surf zone sandbars [e.g., Garnier *et al.*, 2008, 2010; Tiessen *et al.*, 2011; Smit *et al.*, 2012; Castelle *et al.*, 2012; Price *et al.*, 2013]. However, the common characteristic of all these models is that they do not properly account for cross-shore sediment transport processes. For instance, the models of Garnier *et al.* [2008] and Castelle *et al.* [2012] use a basic state approach that assumes that the cross-shore sand transport driven by wave nonlinearities and undertow is in *balance* with the gravitational downslope transport for a given equilibrium (initial) cross-shore beach profile. Although such approach allows the saturation of the growth of the 3-D patterns and, as a result, the detailed investigation of their nonlinear behavior, it has a number of drawbacks. The basic state approach is not compatible with time-varying tide and wave conditions, therefore limiting the applicability of such models to real beaches [Price *et al.*, 2013]. In addition, such models can simulate the downstate LBT-TBR or LBT-RBB sequence but cannot simulate the LBT-RBB-TBR sequence as the onshore sandbar migration is inhibited. Only Ranasinghe *et al.* [2004] simulated the RBB-TBR-LTT transition, although in two separate simulations (RBB-TBR and TBR-LTT). However, strongly obliquely incident waves were required for the latter transition to smooth out the 3-D patterns, while such a transition has been widely observed in the field under normally incident wave conditions [e.g., Price and Ruessink, 2011].

Beach profile models are now able to simulate cross-shore sandbar migration with fair skill on the timescales from hours to months and even years [e.g., Elgar *et al.*, 2001; Hoefel and Elgar, 2003; Ruessink *et al.*, 2007; Kuriyama, 2012; Walstra *et al.*, 2012; Dubarbier *et al.*, 2015; Fernández-Mora *et al.*, 2015]. In these coupled cross-shore “wave flow sediment transport” morphodynamic models, beach profile changes are driven by the *imbalance* between the cross-shore sand transport driven by wave nonlinearities (orbital velocity skewness and asymmetry), undertow, and the gravitational downslope effects. Ruessink *et al.* [2007] showed that rapid (~ 10 m/d) offshore bar migration occurs for storm waves when large waves break on the bar with a dominant offshore bed return flow-induced sediment transport. In between storms, weakly to nonbreaking wave conditions across the bar are associated with a dominant onshore sand transport driven by wave nonlinearities resulting in a slow (~ 1 m/d) onshore sandbar migration. The contribution of near-bed velocity asymmetry to onshore sediment transport was often disregarded in skillful beach profile models [Walstra *et al.*, 2012]. However, the contribution of near-bed velocity asymmetry was sometimes found to be significant [Hoefel and Elgar, 2003], particularly on steep beaches [Ruessink *et al.*, 2016]. To our knowledge, the recent parametrizations of wave nonlinearities [Ruessink *et al.*, 2012] and advances in cross-shore sediment transport using phase-averaged models [e.g., Walstra *et al.*, 2012; Dubarbier *et al.*, 2015; Fernández-Mora *et al.*, 2015] have never been included in 3-D sandbar morphodynamic models.

We hypothesize that 3-D morphodynamic models are not able to simulate the full accretionary behavior of wave-dominated beaches because they overlook cross-shore processes and that including such processes will provide new insight into the mechanisms controlling wave-dominated beach morphodynamics. In this paper, we use a nonlinear morphodynamic 3-D sandbar model (section 2) that includes the recent advances in the cross-shore sand transport contribution. In section 3 the first simulation of a full downstate sequence under time-invariant shore normal waves is described and analyzed. A global analysis is performed to decipher the time evolution of the respective contributions of each process throughout the full downstate sequence. Results are discussed, and conclusions are drawn in section 4.

2. Model and Simulation Setup

2.1. Numerical Model

The nonlinear morphodynamic model is composed of four coupled modules: a spectral wave model, a shortwave-averaged and depth-integrated flow model, an energetic-type sediment transport model, and a bed evolution model. The major difference of this model with the previous version [Castelle *et al.*, 2012] is that the cross-shore sediment transport processes in Dubarbier *et al.* [2015] have been included to remove the basic state assumption. Statistical wave fields are computed from the spectral wave model SWAN (41.10 version) [Booij *et al.*, 1999], using the dissipation model proposed by Ruessink *et al.* [2003] and with quadruplet and triplet interactions switched off. In order to introduce intrawave motions, the model accounts for a robust parametrization of wave skewness as a function of the local wave field [Ruessink *et al.*, 2012]. The contribution of wave asymmetry is disregarded, which will be discussed later in the paper. The bed return flow is

taken into account in the wave radiation stress formulation of *Philipps* [1977] assuming a depth uniform vertical distribution. The phase- and depth-averaged shallow water equations are solved with a pseudo-implicit scheme in order to compute the mean flow field and mean water elevation. The morphological time step is chosen to be longer than the infragravity timescale but significantly shorter than the variations of offshore wave conditions.

The total sediment transport \vec{Q}_t is composed of three modes related to mean flow (\vec{Q}_c), near-bed orbital velocity skewness (\vec{Q}_w), and downslope gravitational effect (\vec{Q}_g). These three modes of transport correspond to the 2-D extension of the formulations detailed in *Dubarbier et al.* [2015] and are defined as

$$\vec{Q}_c = C_c \left[\mathcal{K}_b < |\vec{U}(t)|^2 (\bar{u}_i + \bar{u}_j) > + \mathcal{K}_s < |\vec{U}(t)|^3 (\bar{u}_i + \bar{u}_j) > \right] \quad (1)$$

$$\vec{Q}_w = C_w \left[\mathcal{K}_b < |\vec{u}(t)|^2 \bar{u}(t) \left(\frac{k_i + k_j}{|\vec{k}|} \right) > + \mathcal{K}_s < |\vec{u}(t)|^3 \bar{u}(t) \left(\frac{k_i + k_j}{|\vec{k}|} \right) > \right] \quad (2)$$

$$\vec{Q}_g = C_g \left[\frac{\mathcal{K}_b}{\tan \phi} < |\vec{U}(t)|^3 > + \frac{\mathcal{K}_s \epsilon_s}{w_s} < |\vec{U}(t)|^5 > \right] (\partial_i Z_f + \partial_j Z_f) \quad (3)$$

where the subscript i (j) indicates the cross-shore (alongshore) component, $\phi = 32^\circ$ the friction angle of sediment, ρ the water density, k the wave number, and w_s the sediment fall velocity. $\mathcal{K}_b = \rho \frac{\epsilon_b}{\tan \phi}$ and $\mathcal{K}_s = \rho \frac{\epsilon_s}{w_s}$ are the coefficients linked to bed load and suspended load transport, respectively, with $\epsilon_b = 0.135$ and $\epsilon_s = 0.015$, two numerical coefficients according to *Dubarbier et al.* [2015]. C_c , C_w , and C_g are free friction coefficients. The total velocity field is split into two components, $\vec{U}(t) = \vec{\bar{u}} + \vec{\bar{u}}(t)$, where $\vec{\bar{u}}$ is the time- and depth-averaged mean flow and $\vec{\bar{u}}(t)$ is the orbital velocity defined at the top of the bottom boundary layer. Sediment fluxes are computed at cell centers and further interpolated at the cell interfaces. Sediment can therefore be transferred across the interface between dry and wet cells, although those fluxes are very small, meaning that swash zone processes are not taken into account in the model.

2.2. Model Setup

The initial beach morphology corresponds to a post storm, alongshore uniform, single-barred beach. The morphological characteristics are similar to the observations in *Price et al.* [2013] on the Gold Coast, consisting of a Dean profile that extends offshore to 15.7 m water depth with a superimposed bar located 150 m from the mean sea level shoreline with its crest in 2 m water depth. The computational grid covers a cross-shore distance $L_x = 780$ m and an alongshore distance $L_y = 2000$ m, with a regular grid mesh composed of 10×10 m cells with periodic lateral boundary conditions. Random perturbations with a magnitude of 5 mm were superimposed on the initial bathymetry in order to excite the morphodynamic instabilities. The morphological time step is 1 h.

Constant shore normal swell wave conditions are imposed at the offshore boundary, with a significant wave height $H_s = 1.16$ m, a peak wave period $T_p = 12$ s, and a directional spreading of 20° . The influence of tide is disregarded. A spatially constant d_{50} of 200 μm was used in agreement with the beach sediment at the Gold Coast from which the initial Dean profile is derived [*Price et al.*, 2013]. Preliminary simulations were performed to address the sensitivity of the sandbar response after one morphological time step for a large $C_c - C_w - C_g$ space. The largest variability is observed in the phase space $C_c - C_w$, with the balance between these two coefficients determining if the sandbar migrates onshore or offshore. C_g affects the growth rate of the morphodynamic instabilities, with the growth rate increasing with decreasing C_g . The values were set to $C_c = 0.08$, $C_w = 0.08$, and $C_g = 0.24$ in order to have a full downstate sequence with morphological response times similar to those reported in the literature [e.g., *Ranasinghe et al.*, 2004].

2.3. Global Analysis

A global analysis [*Garnier et al.*, 2010] is used to provide synoptic insight into the contribution of the different processes controlling the morphological downstate sequence. This method is based on the modified bottom evolution equation [*Falqués et al.*, 2000]:

$$\frac{\partial}{\partial t} \left(\frac{1}{2} \|Z_p\|^2 \right) = P_{\vec{Q}_t} \quad (4)$$

where $Z_p = Z_f - \bar{Z}_f$ represents the local bed deviation from the instantaneous alongshore-averaged beach profile \bar{Z}_f . $\|Z_p\| = \frac{1}{L_x L_y} \sqrt{\int_{L_x} \int_{L_y} Z_p^2 dx dy}$ corresponds to the energy of the morphodynamic instability, which

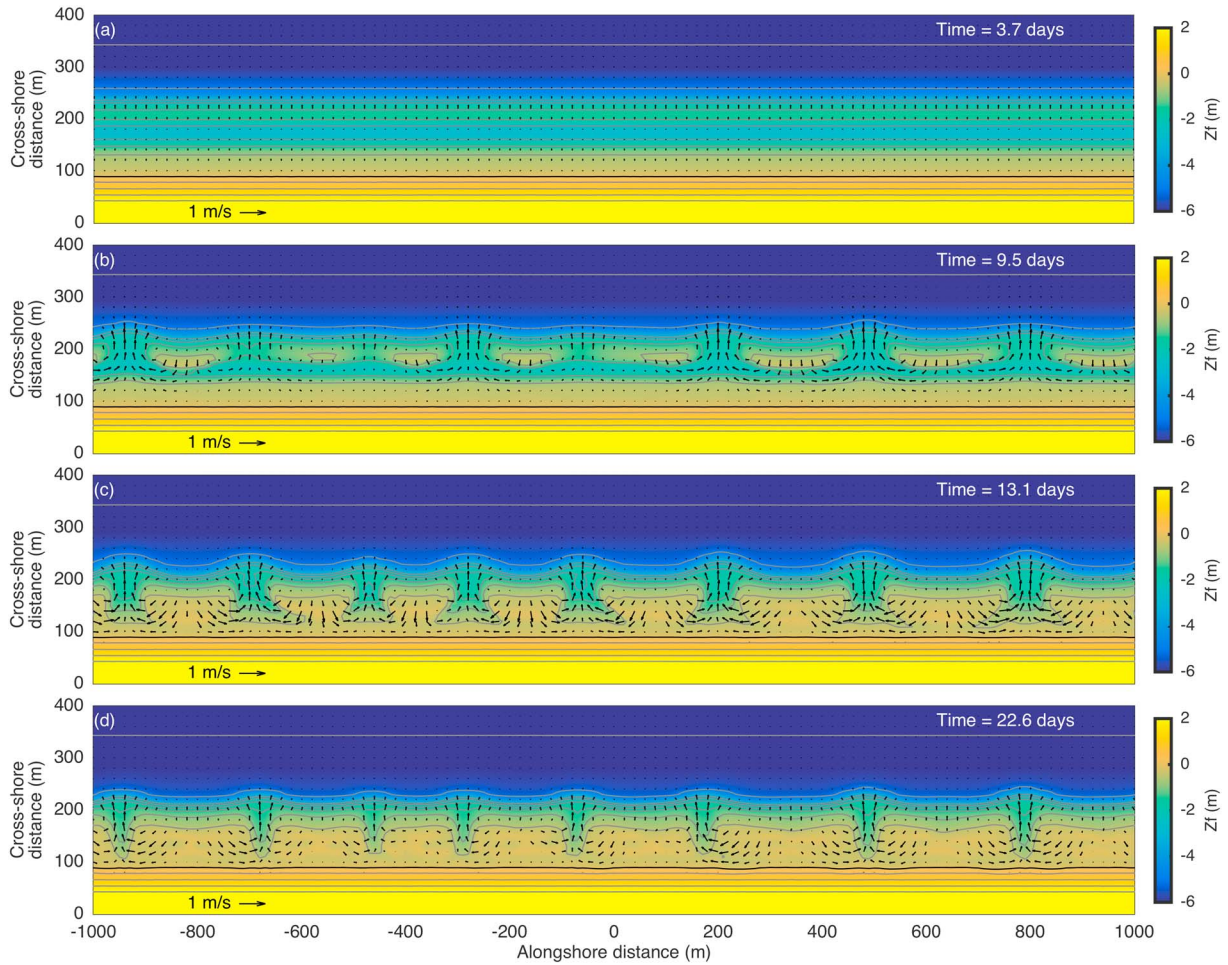


Figure 1. Downstate morphological beach state sequence with superimposed mean flow circulation for a time-invariant wave forcing with $H_s = 1.16$ m, $T_p = 12$ s, and $\theta = 0^\circ$. (a) LBT state at $t = 3.7$ days, (b) RBB state at $t = 9.5$ days, (c) TBR state at $t = 13.1$ days, and (d) LTT state at $t = 22.6$ days. The color bar indicates the seabed elevation with respect to mean sea level (MSL), which is contoured (grey lines), with the black line indicating the MSL shoreline.

is a measure of sandbar three dimensionality. The right-hand side term of equation (4) is the total energy production term, $\mathcal{P}_{\vec{Q}_i} = \mathcal{P}_{\vec{Q}_c} + \mathcal{P}_{\vec{Q}_w} + \mathcal{P}_{\vec{Q}_g}$, from which the production term of each sediment transport mode can be computed as follows:

$$\mathcal{P}_{\vec{Q}_i} = \frac{1}{L_x L_y} \int_{L_x} \int_{L_y} Z_p [\vec{\nabla} \cdot \vec{Q}_i] dx dy \quad (5)$$

with \vec{Q}_i referring to the three sediment transport modes, \vec{Q}_c , \vec{Q}_w , and \vec{Q}_g .

3. Results

Four snapshots of the 30 day downstate LBT-RBB-TBR-LTT simulation are shown in Figures 1a–1d (see Movie S1 in the supporting information for the video showing the continuous evolution), each snapshot showing the beach morphology and superimposed wave-driven currents. Figure 2 shows the corresponding time evolution of the alongshore-averaged beach profile throughout the four intermediate beach states LBT-RBB-TBR-LTT. In section 3.1, the results are analyzed using Figures 1 and 2 for each beach state, with Figure 3a used to objectively define each transition between two beach states as the inflection point of the instantaneous global seabed evolution rate $||\Delta Z_f / \Delta t||$. Figures 3 and 4 are subsequently used in section 3.2 to address the respective contributions of the different sediment transport modes to the beach state evolution.

3.1. Downstate Morphological Sequence

Figure 1a shows the beach morphology during the LBT state at $t = 3.7$ days, which exhibits a continuous deep trough separating the alongshore uniform bar from the beach. Mean currents are essentially offshore

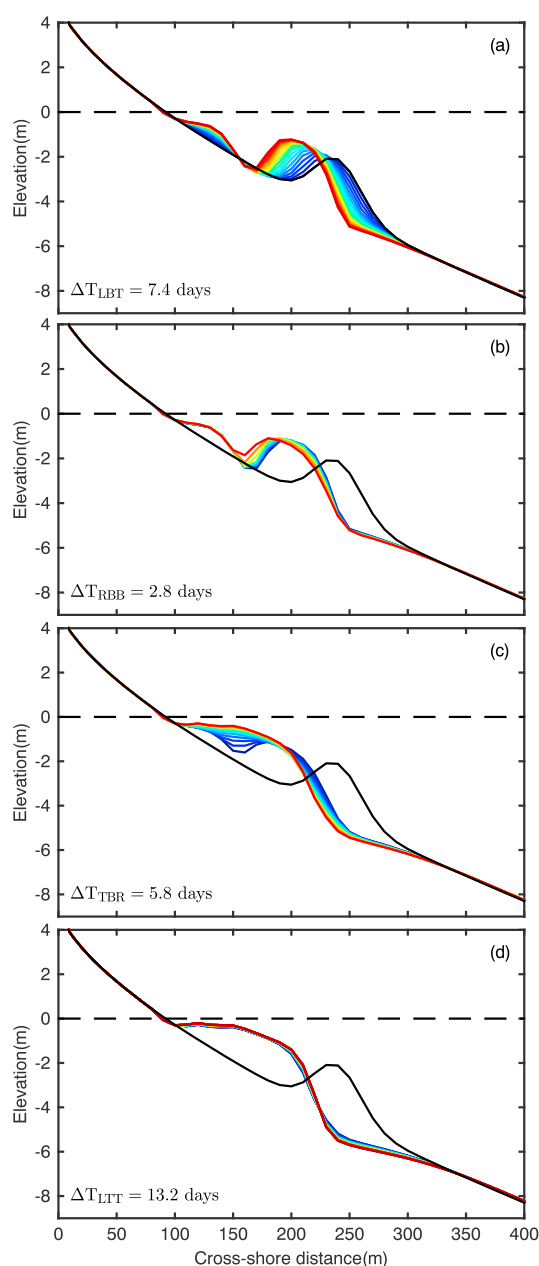


Figure 2. Superimposed alongshore-averaged profiles ($0 < X < 400$ m) during the state (a) LBT, (b) RBB, (c) TBR, and (d) LTT. The time evolution is given by the colors from blue (start) to red (end) every 5 h. In Figures 2a–2d, the initial profile is shown by the black line and mean sea level MSL is indicated by the horizontal black dashed line.

oriented with the maximum intensity localized slightly offshore of the sandbar crest, with the notable absence of circulation. The LBT state lasts 7.4 days and is characterized by an onshore sandbar migration of approximately 40 m, together with an increase in amplitude and a steepening of the shoreward flank (Figure 2a). This behavior is commonly observed during onshore sandbar migration [Ruessink *et al.*, 2007]. Within the LBT state, a progressive decrease in onshore sandbar migration rate from approximately 8 to 4 m/d is observed as the sandbar crest reaches the shallow surf zone, which is in line with the work of Dubarrier *et al.* [2015] and Walstra *et al.* [2013]. This decrease in onshore migration rate explains the decrease in seabed evolution rate $||\Delta Z_f / \Delta t||$ in Figure 3a, while the sandbar remains reasonably uniform alongshore (low $||Z_p||$ throughout LBT in Figure 3b).

The transition LBT to RBB is characterized by the rapid development of morphodynamic instabilities. These bed forms comprise a horn and bay sequence alternating seaward and shoreward of the bar crest resulting in a typical crescentic sandbar morphology (see Figure 1b at $t = 9.5$ days). Rip channels are irregularly spaced alongshore with a variable depth depending on their development stage. The crescentic sandbar development is associated with rip flow circulation, with the most intense rip currents (> 0.4 m/s) flowing through the deepest channels. The evolution within RBB is characterized by an exponential increase in $||Z_p||$ (Figure 3b), which is consistent with earlier surf zone morphodynamic instability modeling [e.g., Garnier *et al.*, 2010; Castelle *et al.*, 2012]. Most of the increase in seabed evolution rate (Figure 3a) is controlled by this increase in beach three dimensionality, although a small amount is also due to the overall onshore sandbar migration (Figure 2b). By the end of the RBB state the sandbar is still detached from the beach and is characterized by the largest seabed evolution rate within the whole LBT-RBB-TBR-LTT sequence (Figure 3a), which is consistent with the laboratory experiment described in Michallet *et al.* [2013].

The transition from RBB to TBR state is characterized by the shallow horn attachment to the beach forming a shore-attached ridge of sand cut by deep rip channels (see the TBR morphology at $t = 13.1$ days in Figure 1c). Compared to the RBB state, the rip channels self-organize in a regular spacing of approximately 250 m with a uniform depth. Rip currents flowing through the channels progressively stabilize to approximately 0.35 m/s in the middle of the TBR state and subsequently slightly decrease in intensity. In agreement with the laboratory results of Michallet *et al.* [2013], the feeder currents and onshore flows across the shallow sandbars are much

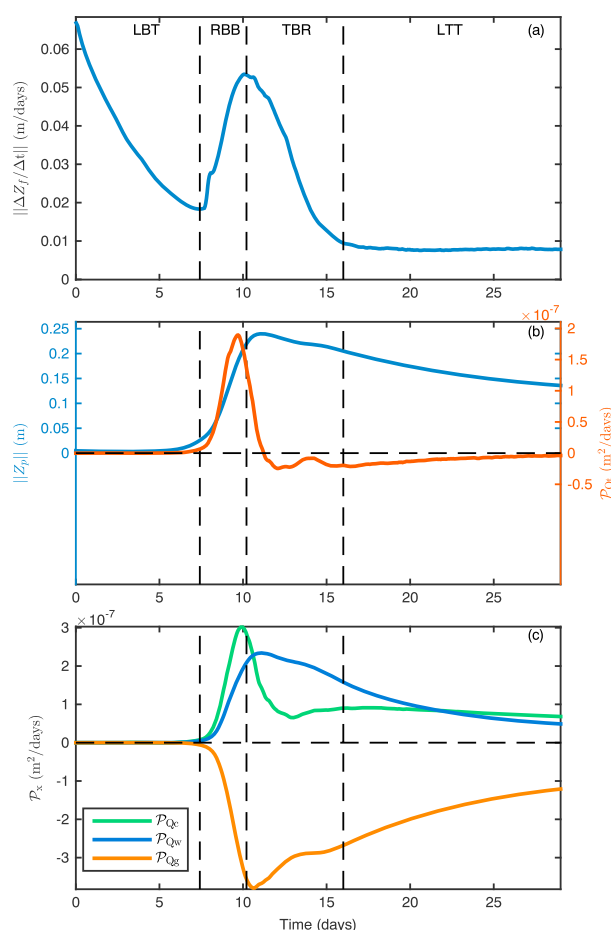


Figure 3. Time evolution of (a) the global instantaneous bed variations rate, (b) the seabed alongshore nonuniformity (blue line) and productivity term relative to the total sediment transport (red line), and (c) productivity terms of each sediment transport mode. The vertical dashed lines indicate the transitions between two consecutive intermediate beach states.

ity parameter (from approximately 0.4 to 1.2, not shown) and increasingly plunging wave breaking, which is in line with *Wright and Short* [1984]. Overall, the morphological evolution description above is the first numerical modeling experiment successfully simulating a full downstate, accretionary, sequence of intermediate beaches. The model outputs can therefore shed light onto the primary driving mechanisms controlling the different stages of the sequence.

3.2. Respective Contributions of the Sediment Transport Modes to Beach State Evolution

The morphological evolution from the late stage of LBT to the early stage of TBR is characterized by positive total production term P_{Q_t} (Figure 3b). This drives a strong increase in beach three dimensionality $||Z_p||$, with a notable exponential growth (linear regime) during the LBT-RBB transition. This increase in beach three dimensionality is primarily driven by the mean flow production term P_{Q_c} (Figure 3c). This is in line with previous works showing that crescentic patterns develop as a result of the positive feedback between rip flow circulation, sediment transport, and seabed evolution [e.g., *Garnier et al.*, 2008]. More surprisingly, while the wave skewness driven sediment transport is the primary mechanism controlling onshore sandbar migration, it also substantially contributes to the increase in beach three dimensionality during the RBB state (see P_{Q_w} in Figure 3c). This contribution notably reflects an additional growth of the horns, although with a lag of less than a day with respect to mean flow sediment transport contribution. In contrast, the gravitational downslope sediment transport systematically acts as a damping term (negative P_{Q_g} in Figure 3c), which is basically proportional to beach three dimensionality $||Z_p||$.

more intense for the TBR state than for the RBB state (Figures 1b and 1c). Sandbar three dimensionality slowly decreases (Figure 3b) as rip channels become progressively shallower and the alongshore-averaged profile becomes increasingly terraced at the end of the TBR state (Figure 2c). This is also in line with the observations of *Brander* [1999] and *Michallet et al.* [2013]. The total evolution rate decreases as the welding of the sandbar to the shore progressively inhibits further onshore migration (Figure 2c).

In contrast with all the other states within the accretionary sequence, LTT is characterized by a quasi-steady morphology as the total evolution rate stabilizes at approximately 0.01 m/d (Figure 3a). This state is characterized by a subtle dynamic equilibrium as the shallow channels merge and split on long timescales (>20 – 30 days, not shown), presumably as a result of the periodic lateral boundary conditions constraining the intrinsic rip spacing. Rip flow circulation is still observed, although its strength is weaker than for the TBR state. This is consistent with earlier works, which often refer LTT rip currents to as mini rips [e.g., *Wright and Short*, 1984], which was subsequently corroborated in the laboratory [*Michallet et al.*, 2013].

The whole downstate sequence is characterized by an onshore sandbar migration (Figure 2). This results in a progressive narrowing of the surf zone and, in turn, a quasi-monotonic increase of the surf similarity

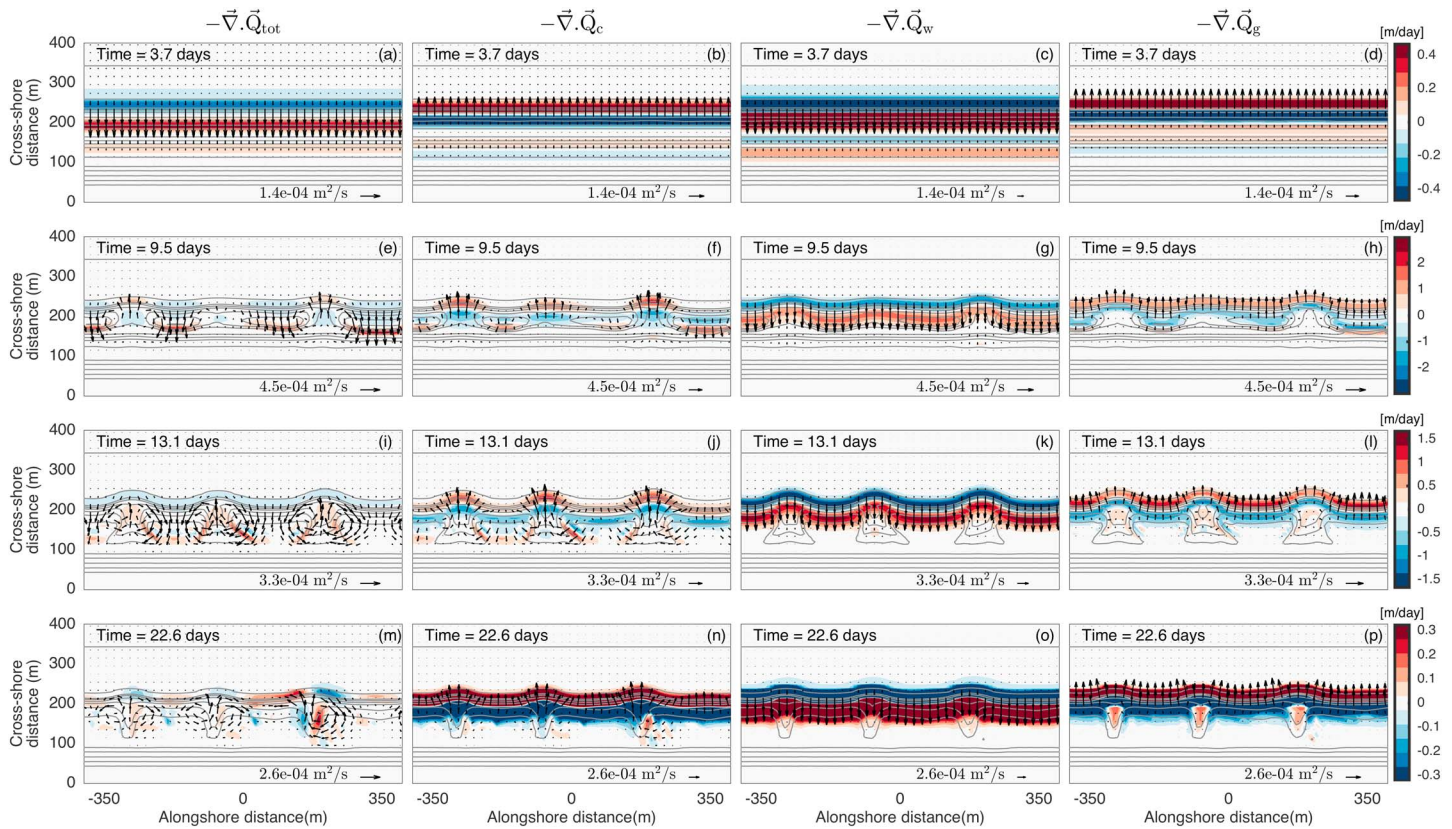


Figure 4. Zoom onto $-400 \text{ m} < Y < 400 \text{ m}$ of the erosion/accretion patterns driven by the total sediment transport and by the different sediment transport modes, with the arrows indicating the sediment fluxes. (a–d) LBT state at $t = 3.7$ days, (e–h) RBB state at $t = 9.5$ days, (i–l) TBR state at $t = 13.1$ days, and (m–p) LTT state at $t = 22.6$ days. The color bar indicates the vertical change in seabed elevation in m/d. The seabed elevation is contoured (grey lines), with the black line indicating the MSL shoreline.

The total production term starts to decrease at the end of the RBB state as a result of the continuous increase in the damping action of the gravitational downslope transport, which is not balanced as a result of a decrease in the mean flow production term $\mathcal{P}_{\bar{Q}_c}$ and a decelerating wave skewness production term $\mathcal{P}_{\bar{Q}_w}$. This change in beach three dimensionality production is concurrent with the shore attachment of the shallow shoreward sections of the sandbar initiating the TBR state. At the early stage of the TBR state, the contributions to beach three dimensionality drastically change, with the wave skewness production term exceeding that of the mean flow. At the same time, the damping action of the gravitational downslope sediment transport overwhelms the wave skewness and mean flow production actions (Figure 3c). This results in a negative total production term and a decrease in beach three dimensionality at the early stage of the TBR state (Figure 3b). During the quasi-steady LTT state, the mean flow and wave skewness production terms become similar, with a slightly larger gravitational downslope damping action (Figure 3c) inhibiting any further growth of beach three dimensionality.

Figure 4 provides insight into the spatial contributions of the three sediment transport modes in the middle of the four intermediate beach states. During the LBT state (Figures 4a–4d), the sediment transport is essentially cross-shore oriented and dominated by the onshore contribution of wave skewness \bar{Q}_w (Figure 4c). This transport mode is not balanced by the undertow-driven (Figure 4b) and downslope (Figure 4d) offshore transport and drives the rapid onshore sandbar migration (Figure 2a). During the RBB state, which is characterized by a positive feedback mechanism driving the development of crescentic patterns (Figure 1b), the seabed evolution is clearly characterized by an accretion and erosion sequence alternating seaward and shoreward of the bar crest (Figure 4e). These patterns are primarily caused by the mean flow driven sediment transport \bar{Q}_c (Figure 4f), while \bar{Q}_w and \bar{Q}_g nearly balance (Figures 4g and 4h). Erosion/accretion patterns dramatically change during the TBR state (Figure 4i), which is characterized by a negative feedback mechanism where beach three dimensionality continuously decreases (Figure 3b) with accretion in both the feeder and rip

channels. Interestingly, accretion of the feeder channels is controlled by the mean flow driven sediment transport, while accretion in the rip channel is controlled by wave skewness driven sediment transport (Figure 4k), with also a notable contribution of the downslope effects (Figure 4l). Finally, during the LTT sequence, erosion/accretion patterns are still clearly observed (Figure 4m) as a result of a subtle imbalance between the three sediment transport modes. Averaging alongshore, the total erosion/accretion patterns give a no-change evolution, as evidenced by the quasi-steady terrace (Figure 2d), because most of the changes are related to the alongshore migration of the channels that try to self-organize into an alongshore uniform feature. The significant productivity terms during the LTT state (Figure 3c) are therefore hypothesized to be artificially increased owing to the periodic lateral boundary conditions.

4. Discussion and Conclusions

Our numerical modeling experiment of a full downstate beach sequence shows morphological changes essentially in line with observations [e.g., *Wright and Short, 1984; Brander, 1999*] and corroborates *Michallet et al. [2013]* in suggesting that overlooking the contribution of cross-shore sediment transport, namely, the imbalance between the sediment transport driven by the undertow, wave skewness, and gravitational downslope effects, was a major impediment to simulate beach state sequences. Clearly, the onshore sediment transport driven by wave skewness controls the onshore sandbar migration throughout the downstate sequence (Figure 2). It also helps the welding of the crescent shoals to the beach. The onshore sandbar migration progressively decreases in rate through the downstate sequence, until a balance is reached between the sediment transport driven by the undertow (Figure 4n), wave skewness (Figure 4o), and the gravitational downslope effects (Figure 4p). Wave skewness driven transport also contributes to an overall increase in beach three dimensionality (Figure 3c). For instance, additional simulations switching off this transport mode at the transition RBB-TBR ($t = 10.2$ days) result in an unrealistic sandbar behavior with the rip-channeled morphology being progressively smoothed out as the bar decreases in amplitude. Wave skewness driven sediment transport is also locally important to the TBR-LTT transition as it favors the shallowing of the rip channels. Accordingly, near-bed orbital velocity skewness must be carefully taken into account in the morphodynamic models of wave-exposed coasts, particularly during beach recovery periods. As such, the further development of improved parametrizations of wave nonlinearities inside and outside the surf zone must be pursued [e.g., *Rocha et al., 2017*].

Another important sediment transport mode is that resulting from the downslope gravity effect that systematically acts as a damping term for beach three dimensionality (see negative $\mathcal{P}_{\bar{Q}_g}$ in Figure 3c). As shown in Figure 4, \bar{Q}_g primarily balances the wave skewness driven sediment transport \bar{Q}_w , although gravitational downslope sediment transport increasingly contributes to the rip channel shallowing when approaching the quasi-steady LTT state (Figure 4l,p). This is in agreement with the field experiment involving the digging of an artificial surf zone channel described in *Moulton et al. [2014]*. The authors demonstrated the key role of downslope gravitational transport mechanism in smoothing out the out-of-equilibrium channel. Given the lack of 3-D morphological diffusivity measurements due to the challenge of experimenting in the natural system, developing laboratory experiments to further improve the parametrization of diffusivity in morphodynamic models is required.

The full downstate sequence can be divided into two different morphodynamic subsequences: (1) the LTT-RBB-TBR sequence characterized by a positive feedback mechanism driving a rapid increase in beach three dimensionality and (2) the TBR-LTT sequence characterized by a negative feedback mechanism driving a decrease in beach three dimensionality toward a quasi-steady beach state. The simulation of the LTT-RBB-TBR sequence corroborates earlier work [e.g., *Garnier et al., 2008*] showing that the increase in beach three dimensionality is mostly driven by the positive feedback between wave-driven rip flow circulation, sediment transport, and the evolving bathymetry. In addition, our simulations demonstrate that wave skewness also contributes to the increase in beach three dimensionality. The respective contributions of the different sediment transport modes during the TBR-LTT sequence are more complicated. As the crescent horns weld to the shore to form a TBR system, beach three dimensionality decreases as a result of the infilling of the rip channel system. Once again, wave skewness driven sediment transport is critical to this sequence as it drives the shallowing of the rip channels, while the feeder channels infill as a result of the mean flow circulation.

There are a number of model limitations in our study. Forcing at the wave group scale and the 3-D structure of nearshore circulation was neglected. More importantly, the sediment transport mode related to

wave asymmetry was not included. This process is known to further enhance onshore sediment transport [e.g., Hoefel and Elgar, 2003; Van Maanen et al., 2008; Dubarbier et al., 2015; Fernández-Mora et al., 2015; Ruessink et al., 2016], although to a smaller extent compared to wave skewness. However, while successfully simulating the LBT-RBB-TBR-LTT sequence, including wave asymmetry sometimes resulted in numerical instabilities in shallow water when reaching the LTT state (not shown). Prior to the LTT state the simulated morphological changes are, however, very similar to those without velocity asymmetry. Detailed field measurements of near-bed velocity skewness and acceleration driven sediment transport are required to robustly address the respective contributions of skewness and asymmetry in the model and to further limit these numerical instabilities. At this stage, it is important to indicate that disregarding wave asymmetry in this study does not mean that it is not a relevant process to beach state sequences. On real beaches, the LBT-RBB-TBR-LTT sequence is systematically associated with a steepening of the subaerial beach [Wright and Short, 1984], which was not reproduced by the model (Figure 2). This drawback is presumably due to the omission of swash zone processes, and at this stage it remains unclear to what extent this omission steers the development of the LTT state. Finally, our model is also supposed to handle erosive up state sequences driven by high-energy storm waves or energetic waves with a large angle of incidence, where rapid offshore migration and reshaping the sandbar into an alongshore uniform feature are observed [e.g., Price and Ruessink, 2011]. This will be explored in a future study.

Additional simulations (not shown) were performed to address the influence of sediment size and wave characteristics. For instance, these simulations show that morphodynamic instability growth rate increases with both decreasing directional spreading and decreasing grain size, although the overall rip spacing is not affected. Although up state sequences were not addressed here, simulations starting from the initial LBT state but with storm wave conditions did not show any onshore sandbar migration. For instance, a slight offshore sandbar migration with a decay in amplitude was simulated for obliquely incident storm waves with $H_s = 4$ m, a peak wave period $T_p = 8$ s, and an angle of incidence of 40° . Other simulations show that for the same wave conditions as those used in the full downstate sequence presented here, but increasing H_s from 1.16 m to 2 m, the model simulates an accretive downstate sequence that does not reach the LTT state. Instead, the model converges toward a TBR morphology with deep rip channels and intense rip currents. This is in agreement with existing observations and with the model of [Wright and Short, 1984] showing that LTT state on similar beaches can only be observed after a sustained period of low-energy waves. An important next step will be to apply the model to real beaches where time-varying wave and tide conditions challenge morphodynamic models. The popularization of video remote sensing systems [Holman and Stanley, 2007] and depth inversion techniques [Holman et al., 2013] appear a promising avenue to provide relevant data sets on surf zone morphological evolution, which are currently sorely lacking for model development and validation.

Most of previous 3-D surf zone sandbar modeling experiments did not properly account for cross-shore sediment transport or used a basic state approach that assumes that the cross-shore transport driven by wave nonlinearities and undertow is in balance with the gravitational downslope transport for a given equilibrium cross-shore beach profile. Here the imbalance between these cross-shore sediment transport processes is found to be critical to the morphodynamics of 3-D surf zone sandbars. Not only does this imbalance drives the alongshore-averaged cross-shore sandbar behavior but it also has a profound impact on beach three dimensionality. The morphodynamic model developed here meets the challenge to integrate the process-based models focusing on cross-shore migration and those working on alongshore variability, which paves the gap to simulate the morphodynamics of real beaches.

Acknowledgments

This work was financially supported by the Agence Nationale de la Recherche (ANR) through the project CHIPO (ANR-14-ASTR-0004-01) and by the INSU/EC2CO AT DRIL (DECA). The movie of the downstate sequence as well as the model outputs used to plot the four figures are provided as supporting information of this paper. The whole model outputs can be provided on demand to B.D. (benjamin.dubarbier@u-bordeaux.fr). Computer time for this study was provided by the computing facilities MCIA (Mésocentre de Calcul Intensif Aquitain) of the University of Bordeaux and the University of Pau and Pays de l'Adour. G.R. acknowledges funding by the Dutch Technology Foundation STW that is part of the Dutch Organisation for Scientific Research (NWO) and which is partly funded by the Ministry of Economic Affairs, under contract 12686 (Nature Coast, S1 Coastal Safety). Two anonymous reviewers are gratefully acknowledged for their constructive comments.

References

- Booij, N., R. C. Ris, and L. H. Holthuijsen (1999), A third-generation wave model for coastal regions: 1. Model description and validation, *J. Geophys. Res.*, *104*(C4), 7649–7666.
- Brander, R. W. (1999), Field observations on the morphodynamic evolution of a low-energy rip current system, *Mar. Geol.*, *157*, 199–217.
- Castelle, B., V. Marieu, G. Coco, P. Bonneton, N. Bruneau, and B. G. Ruessink (2012), On the impact of an offshore bathymetric anomaly on surf zone rip channels, *J. Geophys. Res.*, *117*(F01038), doi:10.1029/2011JF002141.
- Castelle, B., T. Scott, R. Brander, and R. McCarroll (2016), Rip current types, circulation and hazard, *Earth Sci. Rev.*, *163*, 1–21.
- Castelle, B., S. Bujan, S. Ferreira, and G. Dodet (2017), Foredune morphological changes and beach recovery from the extreme 2013/2014 winter at a high-energy sandy coast, *Mar. Geol.*, *385*, 41–55.
- Dalrymple, R. A., J. H. MacMahan, A. J. H. M. Reniers, and V. Nelko (2011), Rip currents, *Annu. Rev. Fluid Mech.*, *43*, 551–581.
- Dubarbier, B., B. Castelle, V. Marieu, and B. G. Ruessink (2015), Process-based modelling of beach profile behavior, *Coastal Eng.*, *95*, 35–50.
- Elgar, S., E. L. Gallagher, and R. T. Guza (2001), Nearshore sandbar migration, *J. Geophys. Res.*, *106*, 11,623–11,627.
- Falqués, A., G. Coco, and D. A. Huntley (2000), A mechanism for the generation of wave-driven rhythmic patterns in the surf zone, *J. Geophys. Res.*, *105*, 24,071–24,088.

- Fernández-Mora, A., D. Calvete, A. Falqués, and H. E. de Swart (2015), Onshore sandbar migration in the surf zone: New insights into the wave-induced sediment transport mechanisms, *Geophys. Res. Lett.*, **42**, 2869–2877, doi:10.1002/2014GL063004.
- Garnier, R., D. Calvete, A. Falqués, and N. Dodd (2008), Modelling the formation and the long-term behavior of rip channel systems from the deformation of a longshore bar, *J. Geophys. Res.*, **113**(C07053), doi:10.1029/2007JC004632.
- Garnier, R., N. Dodd, A. Falqués, and D. Calvete (2010), Mechanisms controlling crescentic bar amplitude, *J. Geophys. Res.*, **115**(F02007), doi:10.1029/2009JF001407.
- Hoefel, F., and S. Elgar (2003), Wave-induced sediment transport and sandbar migration, *Science*, **299**, 1885–1887.
- Holman, R., N. Plant, and T. Holland (2013), CBATHY: A robust algorithm for estimating nearshore bathymetry, *J. Geophys. Res. Oceans*, **118**, 2595–2609, doi:10.1002/jgrc.20199.
- Holman, R. A., and J. Stanley (2007), The history and technical capabilities of argus, *Coastal Eng.*, **54**, 477–491.
- Kuriyama, Y. (2012), Process-based one-dimensional model for cyclic longshore bar evolution, *Coastal Eng.*, **62**, 48–61.
- MacMahan, J. H., E. B. Thornton, and A. J. H. M. Reniers (2006), Rip current review, *Coastal Eng.*, **53**, 191–208.
- Michallet, H., B. Castelle, E. Barthélemy, C. Berni, and P. Bonneton (2013), Physical modeling of three-dimensional intermediate beach morphodynamics, *J. Geophys. Res. Earth Surf.*, **118**, 1–15, doi:10.1002/jgrf.20078.
- Moulton, M., S. Elgar, and B. Raubenheimer (2014), A surf zone morphological diffusivity estimated from the evolution of excavated holes, *Geophys. Res. Lett.*, **41**, 4628–4636, doi:10.1002/2014GL060519.
- Philipps, O. M. (1977), *The Dynamics of the Upper Ocean*, Cambridge Univ. Press, New York.
- Price, T. D., and B. G. Ruessink (2011), State dynamics of a double sandbar system, *Cont. Shelf Res.*, **31**, 659–674.
- Price, T. D., B. Castelle, R. Ranasinghe, and B. G. Ruessink (2013), Coupled sandbar patterns and obliquely incident waves, *J. Geophys. Res. Earth Surf.*, **118**, 1677–1692, doi:10.1002/jgrf.20103.
- Ranasinghe, R., G. Symonds, K. Black, and R. Holman (2004), Morphodynamics of intermediate beaches: A video imaging and numerical modelling study, *Coastal Eng.*, **51**, 629–655.
- Rocha, M., H. Michallet, and P. Silva (2017), Improving the parameterization of wave nonlinearities—The importance of wave steepness, spectral bandwidth and beach slope, *Coastal Eng.*, **121**, 77–89.
- Ruessink, B., C. Blenkinsopp, J. Brinkkemper, B. Castelle, B. Dubarbier, F. Grasso, J. Puleo, and T. Lanckriet (2016), Sandbar and beach-face evolution on a prototype coarse sandy barrier, *Coastal Eng.*, **113**, 19–32.
- Ruessink, B. G., D. J. R. Walstra, and H. N. Southgate (2003), Calibration and verification of a parametric wave model on barred beaches, *Coastal Eng.*, **48**, 139–149.
- Ruessink, B. G., Y. Kuriyama, A. J. H. M. Reniers, J. A. Roelvink, and J. A. Walstra (2007), Modeling cross-shore sandbar behavior on the timescales of weeks, *J. Geophys. Res.*, **112**(F03010), doi:10.1029/2006JC000730.
- Ruessink, B. G., G. Ramaekers, and L. C. van Rijn (2012), On the parameterization of the free-stream non-linear wave orbital motion in nearshore morphodynamic models, *Coastal Eng.*, **65**, 56–63.
- Smit, M. W. J., A. J. H. M. Reniers, and M. J. F. Stive (2012), Role of morphological variability in the evolution of nearshore sandbars, *Coastal Eng.*, **69**, 19–28, doi:10.1016/j.coastaleng.2012.05.005.
- Thornton, E. B., J. H. MacMahan, and A. H. Sallenger Jr. (2007), Rip currents, mega-cusps, and eroding dunes, *Mar. Geol.*, **240**, 151–167.
- Tiessen, M. C. H., N. Dodd, and R. Garnier (2011), Development of crescentic bars for a periodically perturbed initial bathymetry, *J. Geophys. Res.*, **116**(F04016), doi:10.1029/2011JF002069.
- Van Maanen, B., P. J. de Ruiter, G. Coco, K. R. Bryan, and B. G. Ruessink (2008), Onshore sandbar migration at tairua beach (New Zealand): Numerical simulations and field measurements, *Mar. Geol.*, **253**, 99–106.
- Walstra, D. J. R., A. J. H. M. Reniers, R. Ranasinghe, J. A. Roelvink, and B. G. Ruessink (2012), On bar growth and decay during interannual net offshore migration, *Coastal Eng.*, **60**, 190–200.
- Walstra, D. J. R., R. Hoekstra, P. Tonnon, and B. G. Ruessink (2013), Input reduction for long-term morphodynamic simulations in wave-dominated coastal settings, *Coastal Eng.*, **77**, 57–70.
- Wright, L. D., and A. D. Short (1984), Morphodynamic variability of surf zones and beaches: A synthesis, *Mar. Geol.*, **56**, 93–118.